

Alexander Krebs · Christoph Krebs

The Photon Spin - A Natural Constant ?

Measurement Of The Photon Spin
Of Low Energy Photons Of Radio Waves

An English translation from the original German book:
Der Photonenspin - eine Naturkonstante ?
Messung des Photonenspins an energiearmen Photonen von
Radiowellen

Dr. Alexander Krebs Verlag

2014-02-19

Dr. Dr. rer. nat. Alexander Krebs, Dipl.Physiker
Birkenallee 1
74238 Krautheim/Jagst
Christoph Krebs, Dipl.Mathematiker
Graf-Eberstein-Str. 22
74238 Krautheim/Jagst

Bibliografische Information der Deutschen Bibliothek

Die Deutsche Bibliothek verzeichnet diese Publikation in der Deutschen Nationalbibliographie;
detaillierte bibliografische Daten sind im Internet über <http://dnb.ddb.de> abrufbar.

ISBN 978-3-00-026287-6

Dieses Werk ist urheberrechtlich geschützt. Die dadurch begründeten Rechte, insbesondere die der Übersetzung, des Nachdrucks, des Vortrags, der Entnahme von Abbildungen und Tabellen, der Funksendung, der Mikroverfilmung oder Vervielfältigung auf anderen Wegen und der Speicherung in Datenverarbeitungsanlagen, bleiben, auch bei nur auszugsweiser Verwertung, vorbehalten. Eine Vervielfältigung dieses Werkes oder von Teilen dieses Werkes ist auch im Einzelfall nur in den Grenzen der gesetzlichen Bestimmungen des Urheberrechtsgesetzes der Bundesrepublik Deutschland vom 9. September 1965 in der jeweils geltenden Fassung zulässig. Sie ist grundsätzlich vergütungspflichtig. Zuwiderhandlungen unterliegen den Strafbestimmungen des Urheberrechtsgesetzes.

Die Wiedergabe von Gebrauchsnamen, Handelsnamen, Warenbezeichnungen usw. in diesem Buch berechtigt auch ohne besondere Kennzeichnung nicht zu der Annahme, dass solche Namen im Sinne der Warenzeichen- und Markenschutz-Gesetzgebung als frei zu betrachten wären und daher von jedermann benutzt werden dürften.

©2008 Dr. Alexander Krebs Verlag
Krautheim/Jagst
Printed in Germany
Druck: WfB Krautheim

Contents

1	Introduction	2
2	Fundamentals of the macroscopic spin measurement of polarized photons	3
2.1	Theoretical fundamentals	3
2.2	Polarization of the photons of radio waves	4
2.3	Principle of the macroscopic measurement of the photon spin	4
3	Characterization and production of circular polarized radio waves	5
3.1	Characterization of circular polarized radio waves	5
3.2	Generation of circular polarized radio waves	5
3.3	Macroscopic measurement of the photon spin	7
4	Measurement of the photon spin by scattering of a circular polarized radio wave at a small aluminum disc	8
4.1	Angular momentum transference of the radio wave to the small aluminum disc	8
4.1.1	Angular momentum of incident radiation	8
4.1.2	Angular momentum of the scattered radiation	10
4.1.3	Resulting angular momentum of the disc	11
4.2	Rotation of the disc	11
4.2.1	Rotation of the disc under the condition of idealized frictionless motion	11
4.2.2	Rotation of the disc under the influence of friction between water and disc	11
4.2.3	Possible power loss of the scattered radiation	12
4.3	Experimental setup	14
4.4	Analysis	17
4.4.1	Moment of inertia and coefficient of friction of the aluminum disc	17
4.4.2	Determination of the angular momentum effective radiation power on the aluminum disc	18
5	Compilation of the angular momentum effective radiation power density on the aluminum disc of two diverse radio antennas (wave length 2m and 0.7m)	24
6	Calculation of the rotation angle ω of the disc under the assumption of photon spin $h/2\pi$	26
7	Experimental determination of the rotation angle ω of the aluminum disc	28
8	The radiation of satellite antennas and its influence on the attitude dynamics of satellites	30
9	Other kinds of experimental setups	31
9.1	Measurement of angular momentum directly on an actively circularly emitting antenna . .	31
9.2	Measurement of angular momentum on a radiation absorbing disc	31
9.3	Measurement of angular momentum on a thin metal disc by generation of circular polarized radiation by reflection	31
9.4	Measurement of angular momentum on satellites by circular polarized emitting satellite antennas	32
10	Abstract	33
11	Addendum 1: Test records	34

12 Addendum 2	35
12.1 Calculation of the angular momentum of the scattered radiation and the associated reactive opposed angular momentum respectively torsional moment of the scattering disc	35
12.2 Resulting torsional moment on the disc	38
13 Addendum 3	39
13.1 Proof of the equality of the geometrical area of the scattering disc in the photon conception and the effective area of the scattering disc in the electromagnetic wave conception	39
References	42

1 Introduction

According to the particle conception, visible light consists of photons with spin $h/2\pi$. In fact, the spin of visible light can not only be verified by spectroscopic means but also directly by macroscopic measurement of angular momentum. (Such experiments have been conducted especially by R.A. Beth [1] and also by R. Dasgupta and P.K. Gupta [10].)

However, an experimental verification of the photon spin of electromagnetic radiation of very large wave lengths has not yet been accomplished.

Nevertheless today the quantity of the photon spin is considered constant throughout all wave lengths. The question is if the photon spin with growing wave lengths and with a photon mass approaching zero can retain the constant value $h/2\pi$.

For this reason we set ourselves the goal to measure the spin of radio wave photons.

Therefore we also had to use a macroscopic measurement method of the angular momentum (scattering of circular polarized radio waves by a thin aluminum disc), since methods of measurement using atomic physics are not possible at very large wave lengths.

Finally we further refer to the experiments of the past decades with satellites: Presupposed a frequency-independent photon spin there should be observable corresponding angular momentum effects on circular polarized transmitting satellites.

2 Fundamentals of the macroscopic spin measurement of polarized photons

2.1 Theoretical fundamentals

To begin with, every photon according to the present state of knowledge carries the spin respectively angular momentum $s = \frac{h}{2\pi}$ and has the energy $E_p = h\nu$.

We imagine a plane element of area A (lateron infinitely small), through which passes perpendicularly a plane electromagnetic wave of constant intensity.

Hereby conventionally there is applied the term **energy flux density** or **power density** L which indicates how much energy passes through the unit of area in the unit of time.

(Lateron L will be expressed by the Poynting vector.)

Herefrom one can calculate the **photon flux density** P which means the number n of photons which pass through the unit of area in the unit of time at fixed frequency ν :

$$P = \frac{L}{E_p} = \frac{L}{h\nu} \quad (2.1)$$

$$\boxed{\text{photon flux density} = \text{power density} \cdot \frac{1}{h\nu}}$$

From now on we only consider photons having the same spin directions, which corresponds to a circular polarized radiation!

In doing so it's important for us to know, which **total angular momentum** I will be transported during time t through the area by the photons that pass through it. It holds for the absolute value of the angular momentum:

$$I = P \cdot s \cdot t \cdot A = \frac{L}{h\nu} \cdot \frac{h}{2\pi} \cdot t \cdot A = \frac{L}{2\pi\nu} \cdot t \cdot A \quad (2.2)$$

The angular momentum transported by the photons in the unit of time can be described by an **angular momentum flux** J , for which holds: $J = \frac{I}{t} = P \cdot s \cdot A$, also:

$$\boxed{\text{angular momentum flux} = \text{photon flux} \cdot \frac{h}{2\pi}}$$

or accordingly:

$$\boxed{\text{angular momentum flux density} = \text{photon flux density} \cdot \frac{h}{2\pi}}$$

We postulate moreover a photon current which impinges in unit of time perpendicularly on an area A and which will be absorbed or will be emitted perpendicularly by this area.

For this **photon current** F holds: $F = P \cdot A$

Hence it holds for the absolute value of the torsional moment D upon the area, which is caused by the absorbed or emitted photon current:

$$\boxed{\text{torsional moment} = \text{angular momentum flux} = \text{photon flux} \cdot \frac{h}{2\pi}}$$

or:

$$D = \frac{I}{t} = \frac{LA}{2\pi\nu} = F \cdot \frac{h}{2\pi} = P \cdot A \cdot \frac{h}{2\pi} \quad (2.3)$$

2.2 Polarization of the photons of radio waves

The spins of the photons are measurable macroscopically if they add to a collective angular momentum. This requires a polarization of the photons meaning the spins must all have the same direction. In the particle conception a polarized photon radiation corresponds to a circular polarized electromagnetic wave in the wave conception. ([1], [2]).

2.3 Principle of the macroscopic measurement of the photon spin

In order to achieve an additional effect of all photon spins there has to be produced a circular polarized wave by a suited transmitting antenna.

On the one hand the photons of this circular polarized wave when scattered at a thin metall disc can exert an angular momentum on this disc which is accessible to macroscopic measurement.

On the other hand the transmitting antenna experiences the corresponding opposite angular momentum of all the emitted photons, which also is accessible to macroscopic measurement.

3 Characterization and production of circular polarized radio waves

3.1 Characterization of circular polarized radio waves

Two dipoles perpendicular to each other will be activated with sine oscillations of equal intensity and with an angular phase shift of 90° (see Fig. 3.1).

We first inspect the radiation of the dipole system perpendicular to the plane of the system. Superposition of the vectors of the field strengths of both dipoles results in a circular polarized electromagnetic wave ([1], [2], [3], [4], [5]).

When the vectors of the electric field strengths (\vec{E} -vectors) of the emitted wave form a right-handed screw, this wave is called σ^+ -wave.

When conversely the \vec{E} -vectors of the emitted wave form a left-handed screw, then this wave is called σ^- -wave. (σ^- -light).

3.2 Generation of circular polarized radio waves

In our case (Fig. 3.1) the dipoles may be activated in a way that the phase of the horizontal dipole precedes the phase of the vertical dipole by 90° . We first inspect the radiation of the dipole system in the x -direction. Hence the radiation takes place in the manner of a right-handed screw, there is a σ^+ -wave. If one inspects the radiation into the opposite direction ($-x$ -direction) one can see that the radiation takes place in the manner of a left-handed screw (σ^- -wave).

Alltogether it is important that the spin vectors of all the photons are equally oriented in both directions of the radiation of the dipole system. The whole transmitted angular momentum consists consequently of the sum of the spins of all transmitted photons.

Hence according to the law of conservation of angular momentum it can be derived that the circular polarized radiating dipole system or generally every circular polarized radiating antenna must receive the opposite angular momentum of the radiated photons (see chapters 8 and 9).

However, the polarized wave is not only radiated perpendicular to the plane of the dipole system (as schematically presented in Fig. 3.1), but correspondingly to the radiation pattern into all directions.

Depending on the angle of radiation there remains only an elliptical polarization of variable quantity (view chapter 4).

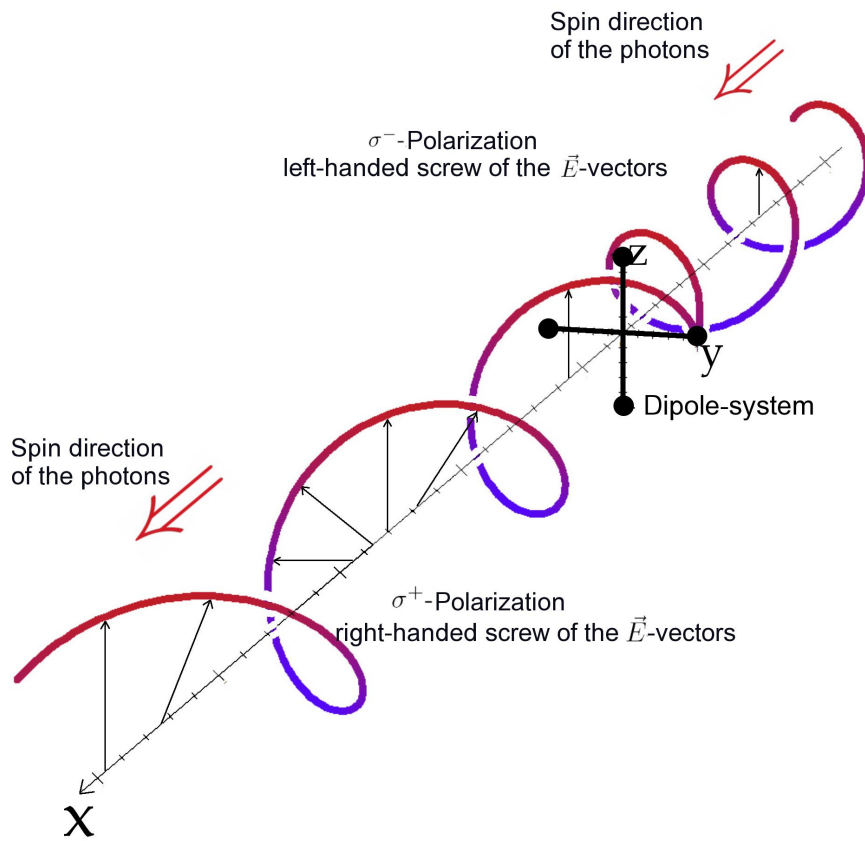


Figure 3.1:
Direction-dependent helicity of the circular polarized radiation of the dipole system

3.3 Macroscopic measurement of the photon spin

In the corpuscular conception the electromagnetic radiation consists of solitary photons with an angular momentum of $h/2\pi$ respectively. A light-beam with σ^+ -polarization has only photons with angular momentum respectively spin-vectors facing in the direction of light propagation, a light-beam with σ^- -polarization has only photons with spin in opposition to the direction of light propagation ([1],[2]). The knowledge of the quantity of the spin and his orientation has almost exclusively been acquired by experiments of atomic physics in the visible and adjacent spectrum by spectroscopy. The only attempt to acquire that knowledge by macroscopic mechanical measurement was the famous work of R.A. Beth [1].

Other than that there have been no further efforts in this respect.

In analogy to Beth's experiment there have been attempts to measure the spin with microwaves, but these experiments were carried out under near-field conditions where only virtual photons exist working like an inductor motor and thus producing meaningless results.

Altogether except Beth's experiments there were no investigations on the photon spin of real free photons in the far field of an electromagnetic wave, especially not with low energy photons at large wave lengths. For instance the photons of $2m$ -UKW-waves (as in our experiment) have an energy and a mass which is only about one billionths of the photons of visible light! Nevertheless by definition (without any experimental verification) they carry the same spin as the photons of visible light.

Finally we further mention an experiment for qualitativ utilization of the photon spin of visible light: An elliptical polarized laser beam is used for angular momentum transfer on micro particles [10].

These were brought to rotation in a fluid under the practical aspect of construction of nano motors.

4 Measurement of the photon spin by scattering of a circular polarized radio wave at a small aluminum disc

A radio wave perpendicularly impinging on a small aluminum disc is scattered at the disc. The configuration of the scattered radio wave depends consequently on the dimension of the scattering disc. When the dimension of the disc is very small compared to the wave length, then the scattered radiation of a linear polarized radio wave has the pattern of a dipole radiation. ([1], [2], [6], [7], [8] and [12]). When the impinging wave is polarized circularly, then the scattered radiation has the radiation of a dipole system of two dipoles perpendicular to each other which are activated with a phase shift of 90° .

Moreover this scattered radiation has equal intensity into the forward and backward direction and the angle distribution of the scattered radiation corresponds to the well known radiation law for dipole antennas.

In our case the diameter of the scattering disc (thin aluminum foil) was 9cm and the wave lengths of the used circular polarized radiation were 2m and 0.7m .

With a relation of disc-diameter to wave length of about 0.04 respectively 0.13 the condition for a scattered radiation according to dipole pattern is fulfilled ([1], [6], [7], [8] und [12]).

4.1 Angular momentum transference of the radio wave to the small aluminum disc

Altogether there acts on the aluminum disc the angular momentum of the incident photons less the angular momentum of the scattered photons (see Fig. 4.1).

The projections of all the spins of the scattered photons onto the plane of the disc cancel mutually (the scattering is rotation symmetric to the axis of the transmitting antenna) so that there remains exclusively an angular momentum perpendicular to the plane of the disc in the direction of the axis of the antenna.

4.1.1 Angular momentum of incident radiation

The geometric conditions for the radiation of the antenna incident on the aluminum disc have been chosen in such a way that the radiation impinges practically perpendicularly and (because of the small diameter of the disc) parallel on the disc.

As usual the radiation is for technical reasons not purely circular polarized, there is rather an elliptical polarized radiation (further details of the transmitting antenna see chapter 5).

In consideration of the ellipticity one can split the radiation into a purely circular and a purely linear part. The circular part then comprises only photons of the same spin orientation perpendicular to the disc.

Annotation:

In the photon conception the intensity of the photons impinging on the disc is determined by its geometrical area A . On the other hand in the electromagnetic wave conception in high frequency technique there is the so called effective area. This fictitious area corresponds to the intensity which the receiving

antenna (in our case the disc) takes out of the electromagnetic wave.

One can show that in our case with our dimensions the geometrical area A of the photon conception is equal to the effective area of the wave conception.

This supports the reliability of our experimental method and setup.

The proof of the equality is rather extensive and omitted here to save space. It can be found in the addendum of this book.

In view of the spatial conditions and the power of the transmitting antenna one can calculate the angular momentum and consequently the torsional moment D_1 which will be transferred from the photons of the antenna onto the disc.

We start with formula 2.2 for the angular momentum which is carried to the disc by the photons in time t :

$$I_1 = \frac{L}{2\pi\nu} \cdot t \cdot A$$

In our case A is the area of the small scattering disc. For the torsional moment follows therefore (because of the constant radiation with respect to time as given in our experiment) from formula 2.3:

$$D_1 = \frac{dI_1}{dt} = \frac{I_1}{t} = \frac{L \cdot A}{2\pi\nu} \quad (4.1)$$

4.1.2 Angular momentum of the scattered radiation

In order to calculate the angular momentum I_2 of the scattered radiation one must know the spin direction and the degree of polarization of the forward and backward scattered photons. We will discuss the rotational directions respectively spin momentum of the photons coming from the antenna and those scattered by the disc.

Let the radiation transmitted by the antenna be $\sigma+$.

Then it holds that the backward scattered radiation has the opposite polarization $\sigma-$. Consequently the spin directions of the incident and the backward scattered radiation are the same in projection on the antenna axis just as with normal reflection (see Fig. 4.1 and chapter 2).

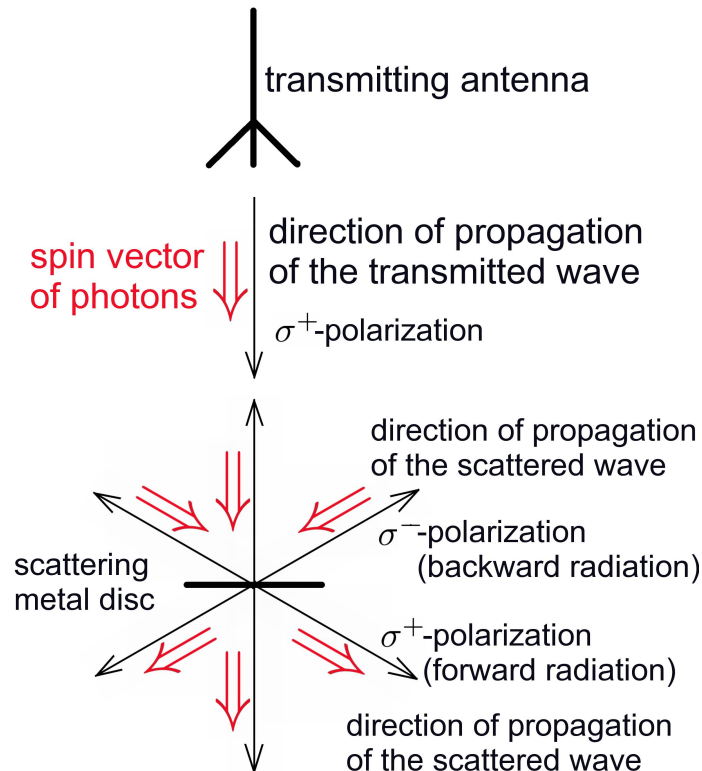


Figure 4.1: Polarization of the scattered radiation

The polarization of the forward scattering wave on the contrary remains unchanged with respect to the polarization of the incident radiation (see chapter 2). Consequently the spin orientation of the forward radiated photons in projection on the antenna axis is the same as the spin orientation of the incident and backward scattered photons in projection on the antenna axis.

Analogous considerations hold for a σ^- -radiation coming from the antenna.

In general it holds:

The spin orientation in projection to the transmitting antenna axis of all involved photons is the same! In order to calculate the angular momentum I_2 one consequently must determine the spin projections on the antenna axis of all scattered photons and weight them with their intensity and their degree of polarization.

This calculation is rather complicated and extensive and can be found in the addendum of this book.

The result is

$$I_2 = \frac{3}{16} \frac{LA}{\pi\nu} \cdot t \quad (4.2)$$

respectively

$$D_2 = \frac{3}{16} \frac{LA}{\pi\nu} \quad (4.3)$$

for the corresponding torsional moment.

4.1.3 Resulting angular momentum of the disc

For the resulting angular momentum I on the disc caused by the incident wave from the antenna less the angular momentum of the scattered photons it holds:

$$I = I_1 - I_2 = \frac{LA}{2\pi\nu} \cdot t - \frac{3}{16} \frac{LA}{\pi\nu} \cdot t$$

Correspondingly there acts the torsional moment D_1 on the aluminum disc caused by the incident photons from the antenna minus the torsional moment D_2 associated with the scattered photons. Hence the resulting torsional moment D of the disc is:

$$D = D_1 - D_2 = \frac{LA}{2\pi\nu} - \frac{3}{16} \frac{LA}{\pi\nu}$$

or

$$\boxed{\text{total torsional moment on the disc } D = \frac{5}{8} \cdot \frac{LA}{2\pi\nu}} \quad (4.4)$$

Annotation:

The experimental method of the measurement of the photon spin by transfer of angular momentum onto a disc floating on water turned out as the only practical method for measuring the spin of radio wave photons. All other methods turned out to be either too accident-sensitive or too unsensitive. Especially thread suspensions were extremely fluttering and not useful. A summary of the diverse tentative methods will be given in chapter 9.

4.2 Rotation of the disc

4.2.1 Rotation of the disc under the condition of idealized frictionless motion

For simplicity we begin with a frictionless supported disc.

The well known formula holds: $D = \Theta \cdot \ddot{\omega}$ with the torsional moment D and the moment of inertia Θ of the aluminum disc.

The integration done twice with the boundary conditions $\omega(0) = 0$ and $\dot{\omega}(0) = 0$ (acceleration from position at rest at time $t = 0$) gives:

$$\omega(t) = \frac{1}{2} \frac{D}{\Theta} t^2 \quad (4.5)$$

Annotation:

This describes also the dynamical situation of a satellite transmitted circular polarized radiation (see chapter 8)!

4.2.2 Rotation of the disc under the influence of friction between water and disc

Previous to the description of our experiments we have to mention that the aluminum disc is situated floating on water under the influence of the radiation of the radio waves to avoid static friction which

(considering the very weak torsional moment of our radiation) could avoid the start of the disc's rotation. (Fluids have no static shear stress.) That means that even arbitrary small torsional moments can induce a rotation of the disc.

Besides this there is only laminar friction, considering the small rotation velocities of the disc, meaning that the friction respectively the torsional moment of the friction is proportional to the rotation velocity.

Determination of the frictional coefficient between water and disc

By means of a little tangential push (see experiment description 4.4.1) the disc is brought to a measurable rotational velocity $\dot{\omega}$.

Subsequently the rotational velocity is recorded by measuring angle ω and time t .

This is a rotational motion whose velocity continually diminishes due to the torsional moment of the friction $-k \cdot \dot{\omega}$:

$$-k \cdot \dot{\omega} = \Theta \cdot \ddot{\omega}$$

After integration done twice:

$$\omega(t) = \frac{\dot{\omega}_0 \cdot \Theta}{k} - \frac{\dot{\omega}_0 \cdot \Theta}{k} e^{-\frac{k}{\Theta} t} \quad (4.6)$$

with boundary conditions $\omega_0 = 0$ und $\dot{\omega}_0 := \dot{\omega}(0)$, so that the angular velocity has its maximum at time $t = 0$.

This formula 4.6 cannot be resolved analytically for k , therefore we calculate numerically.

The necessary experimental data of $\omega(t)$ and t can be experimentally determined (see chapter 4.4, analysis).

Calculation of the rotational angle ω of the disc dependent on time under the influence of torsional moment caused by the circular polarized radio wave and the friction between disc and water

It holds the differential equation:

$$\Theta \cdot \ddot{\omega} = D - k \cdot \dot{\omega} \quad (4.7)$$

with $\Theta \cdot \ddot{\omega}$ = rotation accelerating torsional moment
 D = torsional moment caused by the radio wave
 $k \cdot \dot{\omega}$ = torsional moment caused by friction between disc and water

After integration done twice (see e.g. [11]) we get:

$$\omega(t) = \frac{D\Theta}{k^2} e^{-\frac{k}{\Theta} t} + \frac{D}{k} t - \frac{D\Theta}{k^2} \quad (4.8)$$

with boundary conditions $\omega(0) = 0$ and $\dot{\omega}(0) = 0$.

4.2.3 Possible power loss of the scattered radiation

Not the whole radiation power incident on the disc will be reemitted as scattered radiation. Possible losses are:

a). Ohmic loss (in form of heat)

This can be disregarded because the reflection respectively scattering ability of aluminum with electromagnetic waves beyond infrared is close to 100%.

b). Partial transparency

At first we will consider the $2m$ -wave. The part of the incident power that will penetrate the disc is about 0.25% of the total incident power. Because of the skin effect the penetration depth in aluminum is only $0.006mm$. Due to the much greater thickness of the disc of $0.016mm$ there is therefore a reduction of the current density of 5% for the penetrating radiation, and as the radiation power is proportional to the current density squared there results a coupling of the incident power to the scattered radiation by 99.75%. For the $70cm$ -wave this loss is even smaller due to the higher frequency.

c). Direct reflection as defined by geometrical optics instead of scattering.

Due to the very small dimensions of the disc compared to the wave length (disc-diameter $0.09m$ compared to wave length $2m$ with a relation $1 : 0.045$ respectively to a wave length $0.7m$ with a relation of $1 : 0.13$) the disc scatters the incident radiation like an oscillating dipole system as described in chapter 3.2.

d). Loss of power due to induction of rotation of the disc.

This would be possible if we had had a rotational movement of the disc in our experiments, which however was not the case.

4.3 Experimental setup

In principle the experimental setup consists of an antenna transmitting vertically downwards elliptically respectively circularly polarized radiation on a small aluminum disc floating on water (see Fig. 4.2).

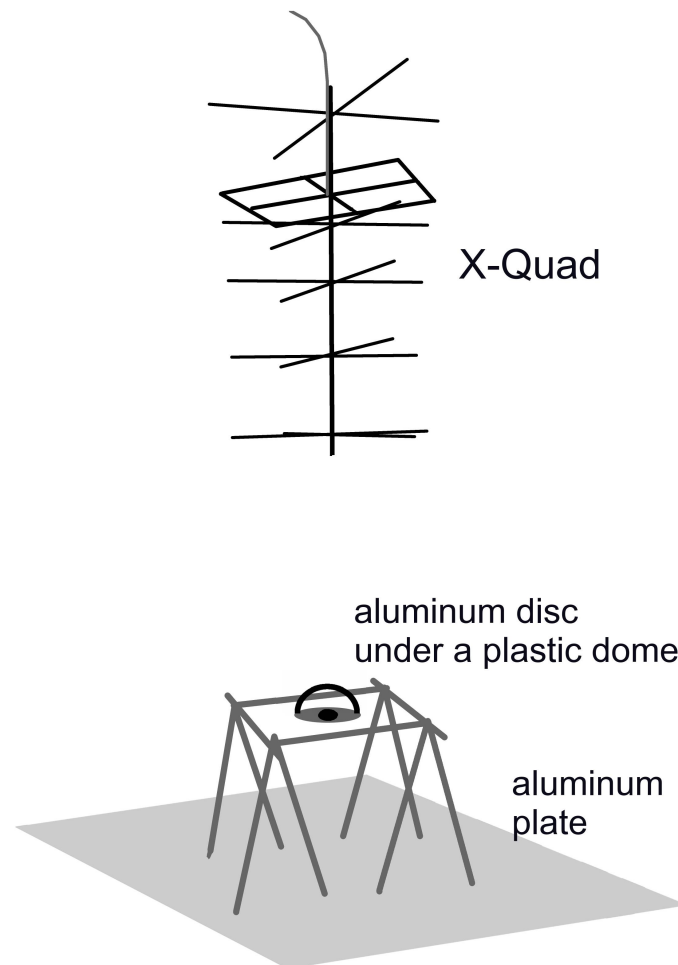


Figure 4.2: Schematic experimental setup

A possible angular momentum transferred by the circular polarized radiation can be recorded by the deflection of a laser beam at a mirror in the center of the aluminum disc (see Fig 4.3). With this one can achieve a sufficient high resolution in measuring the rotational angle of the disc.

For the scattering disc there was used an aluminum foil of thickness 0.016mm , the diameter of the disc is 9cm , the height of the edge 7mm . The disc has a mass of 0.35g .

In addition there is in the center of the disc the mirror with a mass of 0.5g , a breadth of 2cm and a height of 1.7cm .

The electromagnetic wave of the downward transmitting antenna is reflected by the ground producing a standing wave. For optimal reflection the ground has been covered additionally with an aluminum sheet of 2.5m diameter and 1mm thickness.

The used antennas are on the one hand a 2m-X-Quad and on the other hand a 70cm-X-Quad of the firm WiMo - Antennen und Elektronik GmbH.

The former (see Fig. 4.2) with a gain of 10.5dBd , a length of 1.33m and 10 secondary elements.

The latter with a gain of 12.8dBd , a length of 1.13m and 14 secondary elements.

An $X - Quad$ is a hybrid antenna consisting of an active quad-element-system, a reflector and a wave guide system of directors equal to a cross-Yagi (see [13]).

The wave guided along the directors forms at the end of the antenna near the antenna axis an approximately plane wave in the manner of a directed radiation resembling an aperture-type-antenna ([3]).



Figure 4.3: Scattering disc

On grounds of the analogy with the aperture-type-antenna the spacial criteria for the near- and far-field hold likewise for our antenna, especially the criteria for the beginning of the far field region (see [14]). The $X - quads$ were suspended at an arm of $4m$ length. The experiments were carried through in part in a hall and in part in the open air.

As transceiver we have used a Yeasu FT-7800E Transceiver with a power of $40W$ for the $70cm$ -wave respectively $50W$ for the $2m$ -wave.

For the latter there was added an amplifier MICROSET 200SR with $200Watt$ output power (see Fig. 4.4 and 4.5).

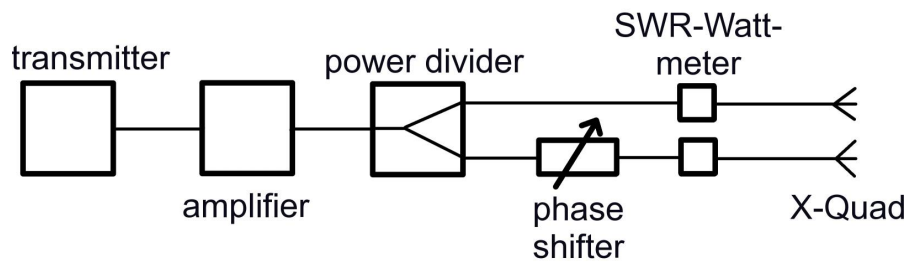


Figure 4.4: Block diagramm

The power partition and the phase shifting in order to produce circular polarized radiation was accomplished by a special device manufactured by the firm WiMo.

The transmitting antenna was connected to the transceiver with a coaxial cable of type RG-213 FOAM with very little loss in order to minimize the power loss at a cable length of $12m$.

The standing wave ratio and the transmission power have been measured by two SWR/Watt-Meter of the manufacturer Daiwa for both antennas of the Quad-system.



Figure 4.5: Electrical assembly

A precise impedance matching has been conducted directly at the elements of the antenna. The scattering aluminum disc was in every case in the far field of the antennas.

For the measurement of the field strength respectively power and the ellipticity of the radiated wave we have used the E - and H -field measurement probes of the firm Schneider - Funk- und Fernmeldetechnik. The aluminum disc lies floating on an about 3mm thick water film within a ceramic plate and is protected against air movement by a transparent plastic dome (Fig. 4.6). It was possible to position the aluminum

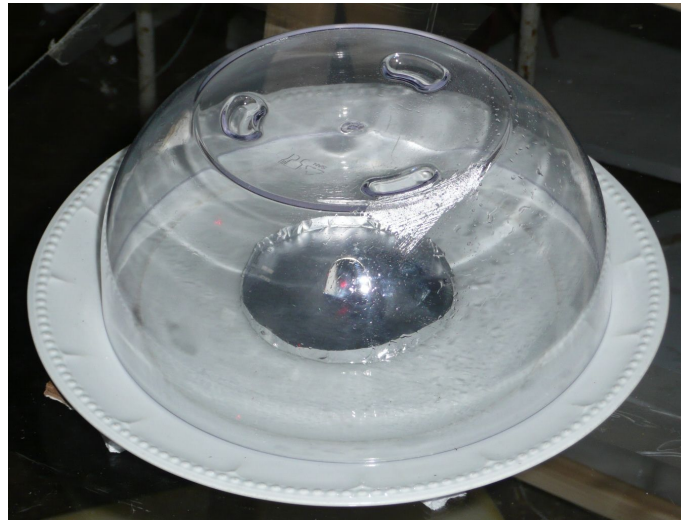


Figure 4.6: Scattering disc with plastic dome

disc manually in the hall due to still air without drifting off during the measurement. In the open air the absolut still positioning of the disc before covering it with the plastic dome was not possible due to constant air movement. Hence the disc was provided with a central hole of about 3mm diameter and was constrained against transversal movement by a vertical metall needle of 1mm diameter in the manner of a roller bearing (but still floating on water). Hereby the determination of the friction coefficient of the disc on water yielded in both cases the same results.

In order to prevent air convection within the dome by warming the air by light irradiation the experiments took place either in the hall with low diffuse light or outside at night.

For damping against external commotions the whole assembly rested on foam plastic caps.

Concerning the distance between transmitting antenna and aluminum disc see the following chapter „Analysis”.

4.4 Analysis

4.4.1 Moment of inertia and coefficient of friction of the aluminum disc

We determine at first the moment of inertia of the disc.

The disc on the whole is provided with a circular edge and a central mirror (see Fig. 4.7). Accordingly

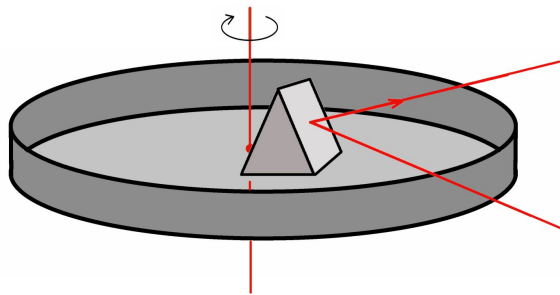


Figure 4.7: Rotating metal disc with mirror

the moment of inertia Θ of the disc can be calculated as $\Theta = 4.9 \cdot 10^{-7} [kg m^2]$.

from the specific mass of the aluminum and the mass and dimensions of the mirror.

Next it is necessary to determine experimentally the friction coefficient k of the disc floating on water.

For this the disc with the mirror was brought to rotation and the rotational angle $\omega(t)$ of the free rotation under the influence of friction was then measured depending on time.

The rotational angle was measured by observation of the laser beam reflected by the mirror. Hereby the rotational velocity has to be chosen sufficiently low to be in the range of a laminar flow. The exact movement is described by formula 4.6:

$$\omega(t) = \frac{\dot{\omega}_0 \cdot \Theta}{k} - \frac{\dot{\omega}_0 \cdot \Theta}{k} e^{-\frac{k}{\Theta} t} \quad [rad]$$

In order to determine k we used an exponential regression based on the recorded data, see Fig. 4.8. For

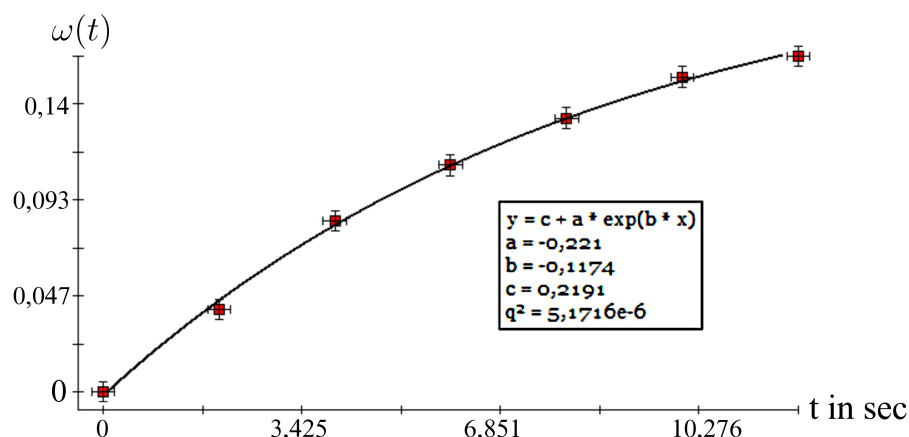


Figure 4.8: Exponential regression, graph of $\omega(t)$

$-\frac{k}{\Theta} = b$ follows the value $-0,117$. Thus it holds

$$k = \Theta \cdot b = 0,117 \cdot 4.9 \cdot 10^{-7} = 5,7 \cdot 10^{-8} \left[\frac{kg m^2}{sec} \right].$$

4.4.2 Determination of the angular momentum effective radiation power on the aluminum disc

Preliminary note 1: Investigation under far field conditions

Our investigation with the aluminum disc has to be carried through imperatively in the far field because only there a measurement of a well-defined angular momentum of the disc under conditions of a correctly orientated energy flux respectively photon flux is possible.

For the far field holds that the vectors of the E -field and the H -field are in phase and perpendicular to each other.

For practical purposes the conditions for the far field given in the technical literature hold in good approximation, especially those given for our type of antennas (see [3], [4], [14], [16] and [15]): $R = 2L^2/\lambda$ Hereby R is the distance of the antenna to the boundary between near and far field (abbreviated far field boundary), L is the maximal geometric dimension of the antenna (in the case of our antenna the length of the antenna) and λ as usually the wave length.

Thus the far field begins in our case for the 70cm wave length antenna at about 3,7m and for the 2m wave length antenna at about 1,7m.

Under those conditions the deviation from the ideal far field is very small, especially in the central region of the main radiation lobe where all measurements were conducted. A good estimate of the deviation from the ideal far field could be accomplished through our measurement of the standing wave over ground as described in the section „Reflection at the ground, production of a standing wave”. We will exemplarily discuss this for the 70cm wave (see Fig. 4.11).

There one can see that the deviation of the minimum (nodal point) of the time averaged energy density of the E -field from the ideal value 0 is about 2%.

(The rotational effect of the electromagnetic wave on our metal disc is proportional to the square of the effective electric field strength and consequently to the time averaged energy density at the plane of the disc at the antinode of the E -field of the standing wave. See for that the legend of Fig. 4.11.)

A further estimate of the far field boundary used by us provides the following fact:

By measuring the effective E -field perpendicular to the disc along the antenna axis from ground to about 1.2m height we could show that this E -field is about 1/10 (one tenth) of the angular-momentum-effective E -field in the plane of the disc perpendicular to the axis of the antenna. Considering the square of the field strength as mentioned above there is a deviation from the ideal conditions (E -field strength in the direction of the axis of the antenna = 0) in the range of 1%. In literature a deviation of 2% or less is considered a good criterion for being in the far field.

Preliminary note 2: Investigation on polarized radiation. Reduction to net circular polarized radiation.

Our antennas produce an elliptic polarized radiation with an ellipticity of about 3dB, that means that the relation of the semi-minor axis to the semi-major axis of the ellipse specified by the electric field vector in the plane perpendicular to the radiation direction is 0.7 : 1.

This is corresponding to the technical literature a very satisfying ellipticity (see [15]). The elliptic polarized radiation can be seen as composed of a purely circular and a purely linear polarized wave.

For further measurement data we will only refer to the angular-momentum-active part of purely circular polarized radiation.

The effective field strength of the circular polarized part corresponds to the semi-minor axis of the polarization ellipse and can be determined easily by measurement.

Accordingly the power of the circular polarized part of the wave is about 2/3 of the whole power of the transmitted radiation.

See also the polarization ellipses of the 2m-wave in figure 4.9, their semi-minor axis corresponding to the purely circular polarized part of the antenna radiation. There have been plotted on the one hand the effective field strength of the electric field (in V/m) and on the other hand the effective field strength of the magnetic field (in A/m) depending on their direction in the plane perpendicular to the radiation direction. The circular polarized part corresponds to a circle plottet inside the ellipse.

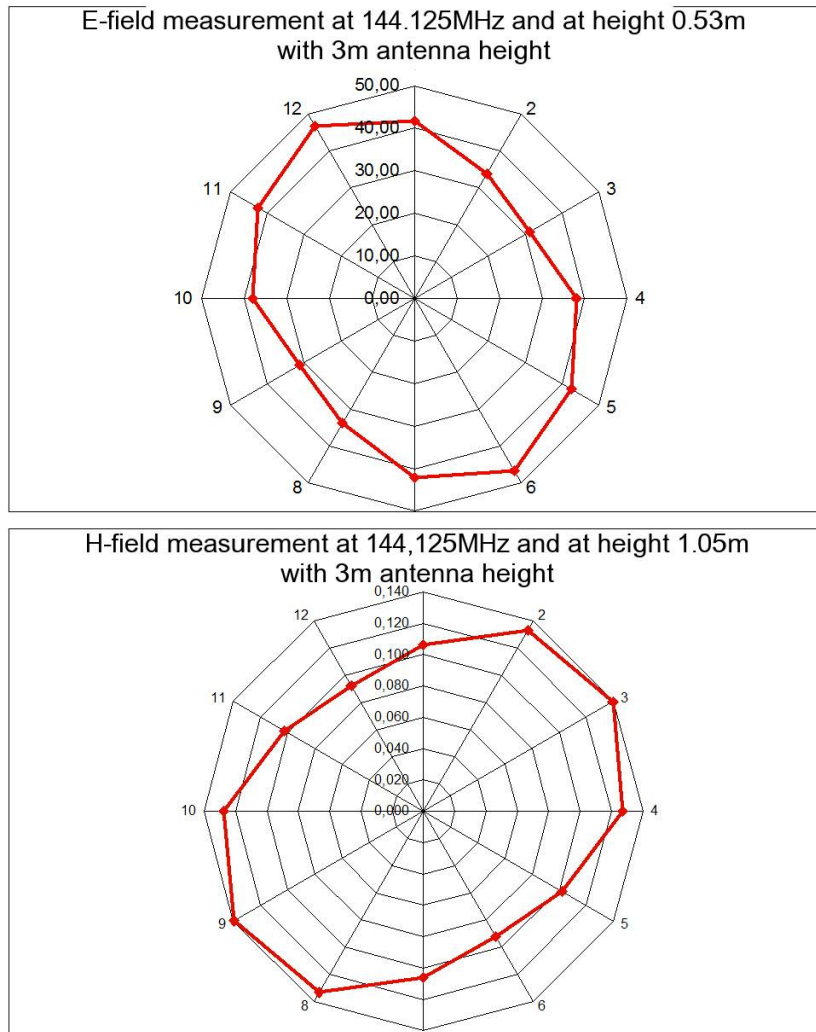


Figure 4.9: Polarization ellipses of the $2m$ -wave. Measurement of the direction dependence of the effective E - and H -field strengths.

Helicity of the circular polarized radiation incident on the disc (see 4.10)

With our setup the aluminum disc receives a radiation from above (from the antenna) and from below (reflected from the ground). It is important that the helicity of the reflected radiation changes compared to the radiation coming from the antenna! If for instance the radiation coming from the antenna is σ^+ , then the helicity of the reflected radiation is σ^- (see Fig. 4.10). That means in the photon conception that the spin orientation of the photons of the wave coming from above and below is the same. Thus the photons of the radiation from above and below can give their angular momentum additionally to the aluminum disc.

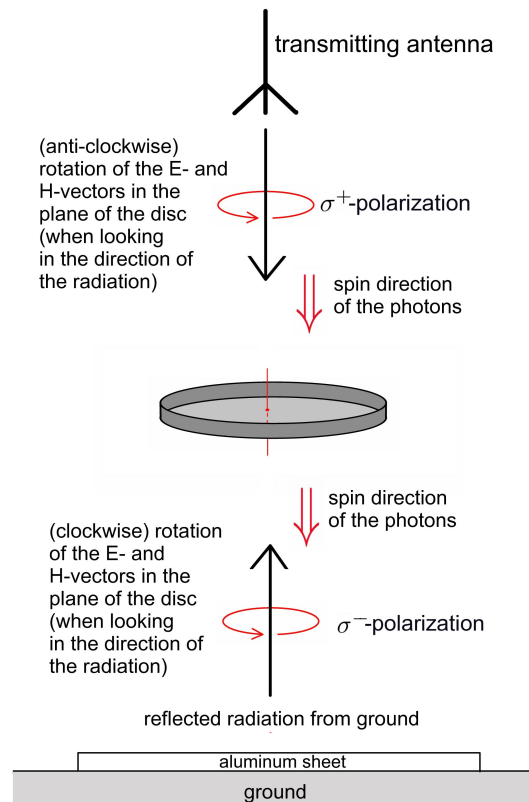


Figure 4.10: Addition of the angular momentum-effective radiation powers of the waves coming from the antenna and from the wave reflected by the ground. In the wave conception coincident rotational direction of the E -field vectors of both waves, in the photon conception coincident spin directions of both radiations.

Reflection at the ground: Production of a standing wave

The radiation of the antenna is orientated perpendicular to the ground (see chapter 4.3 experimental setup). The circular polarized radiation, which is incident perpendicular to the ground (respectively the aluminum plate) is being reflected again as a circular polarized radiation.

Our aluminum disc has a very high reflectivity of nearly 100%. Therefrom by superposition of the downward and upward directed waves there is generated an almost ideal circular polarized standing wave near ground.

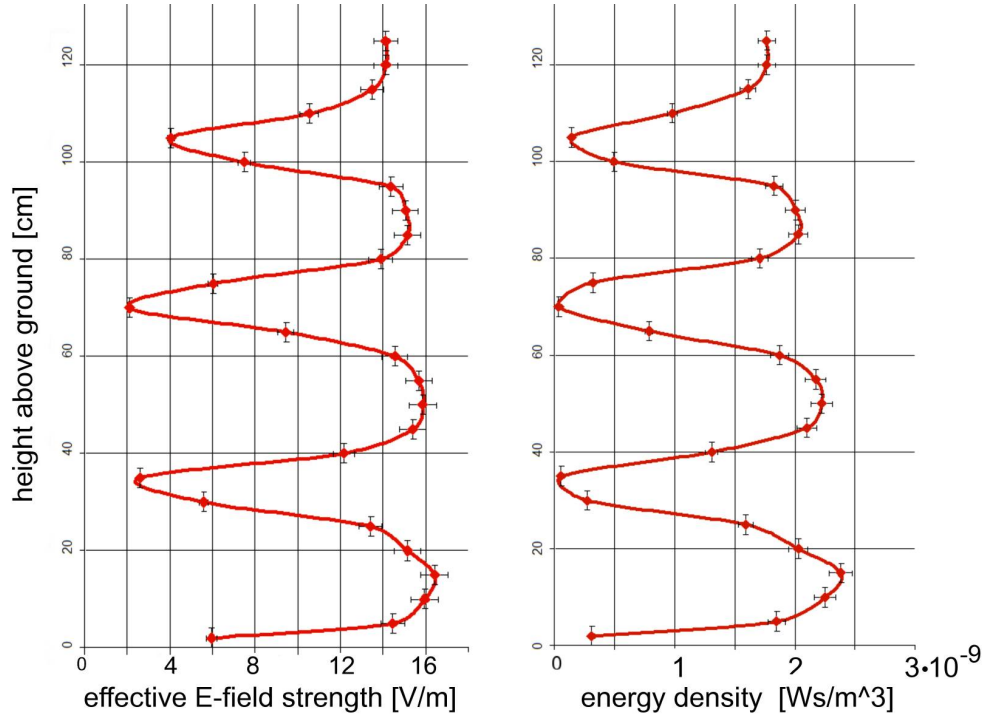


Figure 4.11: The circular polarized standing wave over ground (wave length 68cm). Effective E -field strength and time-averaged energy density of the E -field as a function of the height above ground respectively the metal sheet. (On the left one can see well the basic function of the absolute value of a sine.) Generally it holds for the time-averaged energy density W of the E -field of a plane linear polarized wave: $W = 1/2 \cdot \epsilon_0 \cdot E_{eff}^2$. In the case of a circular polarized wave there is an additional factor 2: $W = \epsilon_0 \cdot E_{eff}^2$ (Height of the antenna above ground 5m , power of the transmitter 40W , frequency 440MHz)

This can be measured easily passing through the field near ground upward with an E -field-test-probe respectively by rotating the test-probe in the different planes parallel to the ground (see Fig. 4.11).

„Near ground” means in our case the altitude range of 1.25m for the 70cm -wave and of 1.75m for the 2m -wave with respect to the ground.

Closer to the antenna the quality of the standing wave decreases because there the strong wave from the antenna meets the lower intensity of the reflected wave from the ground.

For the 70cm -wave the antinode of the E -field respectively the node of the H -field are at $5/4\lambda = 87,5\text{cm}$ above ground. We measured the E -field at this height.

For the $2m$ -wave the antinodes of the H -field respectively of the E -field are at $100cm$ respectively $50cm$ above ground. We measured the E -field and the H -field at this heights.
(Because of the fine-tuning necessary for optimization of the antenna power the exact function parameters of the antennas are slightly shifted with respect to the standard values of the wave lengths of $70cm$ and $2m$. This is especially indicated in Fig. 4.11 and chapter 5).

From the measurement of the field strengths to the determination of the angular momentum -effective radiation power incident on the aluminum disc

With our E -field strength test probe the effective field strength in the planes parallel to the metall disc was being measured.

Because of the standing circular polarized wave we measured in the antinode of the E -field in every direction the same effective field strength.

The H -field here is negligible low, see hereto 4.4.2, preliminary note 1.

The measured effective field strength E_m arises from the superposition of the effective field strengths E_a of the wave coming from the antenna and the effective field strength E_b of the wave reflected from the ground.

Because near ground there is a superposition of the E -field vectors in phase, and due to E_a and E_b having equal strength, the measured field strength E_m is twice the field strengths of E_a and E_b , thus it holds: $E_a = E_b = \frac{1}{2}E_m$

The time averaged power of the radiation causing the angular momentum of the disc cannot be determined by one Poynting vector because the standing wave arises from two waves moving in opposite directions (see [8]).

It is rather necessary to formulate the Poynting vectors of both waves moving in opposite directions separately to calculate the power density delivered to the disc and to add those afterwards.

For an electromagnetic wave generally holds for the Poynting vector: $\vec{S} = \vec{E} \times \vec{H}$

In the special case of a linear polarized wave under far field conditions there is

$$|\vec{S}| = S = E^2/Z_0 = H^2 \cdot Z_0$$

with the time averaged power density S and the effective field strengths E and H .

Hereby Z_0 is the characteristic wave impedance of the vacuum.

We now determine the angular-momentum-effective power density L of the radiation onto the disc.

To begin with we measure in an antinode of the E -field the effective strength E_m of the E -field of a normally linear polarized standing wave. (Since here the H -field has a node, the whole energy is in the E -field.)

The measured E -field strength is the additive supoerposition of the waves coming from above (E_a) and below (E_b), each of them having consequently only half the field strength of E_m , hence: $E_a = E_b = \frac{1}{2}E_m$ (as mentioned above).

Each of both waves has the power density $L = \frac{E^2}{Z_0}$ ($Z_0 = 377\Omega =$ characteristic wave impedance of the vacuum)

Both waves together consequently deliver a power density of

$$L = \frac{E_a^2}{Z_0} + \frac{E_b^2}{Z_0} = \frac{1}{4} \frac{E_m^2}{Z_0} + \frac{1}{4} \frac{E_m^2}{Z_0} = \frac{1}{2} \frac{E_m^2}{Z_0}$$

Now in our case we have two pairs of linear polarized waves, each pair forming a circular polarized wave coming from above and from below generating a standing circular polarized wave.

Based on the fact of the equal magnitude of the resultant field strengths of each pair we finally get the power density

$$L = \frac{E_m^2}{Z_0} \tag{4.9}$$

Analogically it holds for L at the antinode of the H -field:

$$L = H_m^2 \cdot Z_0 \tag{4.10}$$

5 Compilation of the angular momentum effective radiation power density on the aluminum disc of two diverse radio antennas (wave length 2m and 0.7m)

At first the measurement results of the effective field strengths of the circular polarized wave at the respective antinodes are specified. From this according to formulas 4.9 and 4.10 the angular-momentum-effective power densities can be calculated.

See also preliminary note 2 of chapter 4.4.2.

1. For the „70cm” antenna holds:
wave length $\lambda = 68cm$, frequency 441,2MHz

far field boundary at 3.7m
 - a) height of the antenna above ground: 5m
height of the aluminum disc above ground: 85cm
effective strength of the E -field at the antinode at 85cm height: $(5/4\lambda)$: 15.1V/m
Therefrom we get an angular-momentum-effective power density $L = 0.6 W/m^2$.
2. For the „2m” antenna holds:
wave length $\lambda = 210cm$, frequency 144,1MHz
far field boundary at 1,7m
 - a) height of the antenna above ground: 4.5m
height of the aluminum disc above ground: 53cm
effective field strength of the E -field at the antinode at 53cm height: 28V/m
Therefrom we get an angular-momentum-effective power density $L = 2.1 W/m^2$.
 - b) height of the antenna above ground: 4.5m
height of the aluminum disc above ground: 1.05m
effective field strength of the H -field at the antinode at 105cm height: 0.071A/m
Therefrom we get an angular-momentum-effective power density $L = 2.0 W/m^2$.
 - c) height of the antenna above ground: 3m
height of the aluminum disc above ground: 53cm
effective field strength of the E -field at the antinode at 53cm height: 31.6V/m
Therefrom we get an angular-momentum-effective power density $L = 2.7 W/m^2$.

- d) height of the antenna above ground: $3m$
height of the aluminum disc above ground: $1.05m$
effective field strength of the H -field at the antinode at $105cm$ height: $0,092A/m$
Therefrom we get an angular-momentum-effective power density $L = 3.2 W/m^2$.

6 Calculation of the rotation angle ω of the disc under the assumption of photon spin $h/2\pi$

Now all experimentally determined parameters are available for the calculation of ω . The basis of the calculation constitute the formulas 4.8, 12.4, 4.9 and 4.10:

- $\omega(t) = \frac{D\Theta}{k^2} e^{-\frac{k}{\Theta}(t)} + \frac{D}{k} t - \frac{D\Theta}{k^2}$
- Total torsional moment $D = \frac{5}{8} \cdot \frac{LA}{2\pi\nu}$
- $L = \frac{E_m^2}{Z_0}$
- $L = H_m^2 \cdot Z_0$

The parameters are:

- Moment of inertia of the aluminum disc: $\Theta = 4.9 \cdot 10^{-7} \text{ kg m}^2$
- Area of the disc: $A = 6,4 \cdot 10^{-3} \text{ m}^2$
- Friction coefficient between disc and water: $k = 5,7 \cdot 10^{-8} \frac{\text{kg m}^2}{\text{sec}}$
- Radiation time $t = 360 \text{ sec}$

We list the results according to chapter 5:

1. For the 70cm-wave holds:

a) $\nu = 441,2 \text{ MHz}$, $L = 0,6 \frac{\text{W}}{\text{m}^2}$, $D = 8,66 \cdot 10^{-13} \text{ kg m}^2$
 \Rightarrow Rotation after 360 seconds:

$$\omega(360s) = 0,0053 \text{ rad} = 0,3^\circ$$

This corresponds in our case to a deflection of the laser beam of $5.3\text{cm} \cdot 2 = 10.6\text{cm}$ (factor 2 because of the reflection of the laser beam from the mirror).

(Length of the laser beam in each case normalized to 10m.)

2. For the 2m-wave holds:

(a) und (b) $\nu = 144,125 \text{ MHz}$, $L = 2.05 \frac{\text{W}}{\text{m}^2}$ (average),
 $D = 9,06 \cdot 10^{-12} \text{ kg m}^2$
 \Rightarrow Rotation after 360 seconds:

$$\omega(360s) = 0,0558 \text{ rad} = 3,2^\circ$$

This corresponds in our case to a deflection of the laser beam of $55,8\text{cm} \cdot 2 = 111,6\text{cm}$ (factor 2 because of the reflection of the laser beam from the mirror).

(Length of the laser beam in each case normalized to 10m.)

(c) und (d) $\nu = 144,125 \text{ MHz}$, $L = 3,0 \frac{\text{W}}{\text{m}^2}$ (average),
 $D = 1,33 \cdot 10^{-11} \text{ kg m}^2$

\Rightarrow Rotation after 360 seconds:

$$\omega(360s) = 0,082 \text{ rad} = 4,7^\circ$$

This corresponds in our case to a deflection of the laser beam of $81,7\text{cm} \cdot 2 = 163,4\text{cm}$ (factor 2 because of the reflection of the laser beam from the mirror).

(Length of the laser beam in each case normalized to 10m .)

7 Experimental determination of the rotation angle ω of the aluminum disc

Basis for our measurements are the experimental setup for the angular momentum effective power density and the physical parameters as described in chapter 4 and chapter 6.

Again we specify the deflection of the laser beam normalized to $10m$ length of the laser beam and we give the rotational angle ω in angular degrees.

Furthermore there is to account for the deflection of the laser beam at the mirror which doubles the rotational angle with respect to the rotation angle of the disc.

1. For the $70cm$ antenna at $5m$ height above ground there results averaged from 7 separate measurements a deflection of the laser beam of $0.2 cm$.
This corresponds to a rotation angle of the disc of
 $\omega = 0.011^\circ \cdot \frac{1}{2} = 0.0055^\circ$
with a standard deviation $\sigma = 0.21^\circ \cdot \frac{1}{2} = 0.11^\circ$.
(Separate measurements are listet within the addendum.)
2. For the $2m$ antenna at $4.5m$ height above ground there results averaged from 6 separate measurements a deflection of the laser beam of $0.4 cm$.
This corresponds to a rotation angle of the disc of
 $\omega = 0.022^\circ \cdot \frac{1}{2} = 0.011^\circ$
with a standard deviation $\sigma = 0.27^\circ \cdot \frac{1}{2} = 0.14^\circ$.
(Separate measurements are listet within the addendum.)
3. For the $2m$ antenna at $3m$ height above ground there results averaged from 25 separate measurements a deflection of the laser beam of $0.5 cm$.
This corresponds to a rotation angle of the disc of
 $\omega = 0.027^\circ \cdot \frac{1}{2} = 0.014^\circ$
with a standard deviation $\sigma = 0.42^\circ \cdot \frac{1}{2} = 0.21^\circ$.
(Separate measurements are listet within the addendum.)
Especially for the purpose of a very exact statistic in this case there has been conducted a large number of measurements.

In doing so we have used the conventional standard deviation $\sigma = \sqrt{\frac{1}{n} \sum (x_i - \bar{x})^2}$.

To mention it briefly we annotate that a measurement value lies with about 68% probability in the range between $-\sigma$ and $+\sigma$ and with a probability of about 95% in the range of -2σ to $+2\sigma$.

In summary this means:

1. 70cm –antenna at 5m height:
Calculated deflection of the 10m laser beam provided that a photon spin of $h/2\pi$ exists: 10.6cm
Measured deflection: $0.2\text{cm} \pm 4\text{cm}$
2. 2m –antenna at 4.5m height:
Calculated deflection of the 10m laser beam provided that a photon spin of $h/2\pi$ exists: 111.6cm
Measured deflection: $0.4\text{cm} \pm 5\text{cm}$
3. 2m –antenna at 3m height:
Calculated deflection of the 10m laser beam provided that a photon spin of $h/2\pi$ exists: 163.4cm
Measured deflection: $0.5\text{cm} \pm 7\text{cm}$

From this follows:

For the photons with frequency 144MHz and 440MHz respectively the wave lengths 70cm and 2m there is no photon spin of magnitude $h/2\pi$ detectable!

More generally:

On low energy photons in the radio wave range there is no photon spin of magnitude $h/2\pi$ detectable. Especially the experiments with the larger 2m –wave show that the photon spin (if existent) must be far below the magnitude $h/2\pi$.

8 The radiation of satellite antennas and its influence on the attitude dynamics of satellites

The motion of the satellites is described by global orbital dynamics and local attitude dynamics, the latter being generally spoken a description of the diverse angular momentums respectively torques which act on satellites.

Such torsional moments are very interesting to us because satellites are often equipped with circular polarized transmitting antennas. Consequently, if the satellite transmits a circular polarized radio wave, there should be a measurable torsional moment onto the satellite caused by the photon spin, if the spin is indeed $h/2\pi$ independent of the frequency (see chapter 2).

There are however many different kinds of origin for torsional moments on satellites which one has to know to measure the torsional moment of a circular polarized transmitting antenna. For example there are gravitation, radiation pressure (which may also cause a torsional moment on the satellite if the center of mass is not on the transmitting axis), aerodynamic resistance, thermic deformations or solar wind. However all of those are well known and are being measured and compensated for regularly.

For us now there arises the question: Have perturbing torques on satellites been caused by transmission of circular polarized transmitting satellite antennas? And how big would those be with common transmitting powers?

We first assume a circular polarized and approximatively unidirectional transmitting antenna with power $W = 100W$.

Furthermore we assume a common frequency of $1GHz$ (L-band IEEE).

In this frequency range there are numerous circular polarized transmitting communication satellites.

Then the torque D of the antenna (see chapter 2) is $D = \frac{W}{2\pi\nu}$, hence in our case $D = 1.5 \cdot 10^{-8} Nm$.

With less but also common frequencies as for example $0.1GHz$ the perturbing torque even raises to $D = 1.5 \cdot 10^{-7} Nm$.

Both these torques are within the limits of common measurement techniques on satellites and well detectable, so they should have been detected in the past decades!

This becomes especially evident if one considers that e.g. the torsional moment caused by radiation pressure from an off center transmitting antenna, which is about equally strong, is well known and has been measured many times.

We'd also like to mention that those two perturbing torsional moments can hardly be mixed up, because the torque vectors of the two are perpendicular to each other.

Summing up it holds that a torque on a circular polarized satellite antenna resulting from a constant photon spin $h/2\pi$ in any case would have attracted attention long ago. That this didn't happen is a further indication for the assumption of a frequency dependent photon spin.

9 Other kinds of experimental setups

The experimental setup we have presented in chapter 4.3 was not the only and first one we tried for our spin measurement. In fact it was the last one in a large series of experiments of which all preceding ones had turned out to be not practicable or possible in the framework of our financial possibilities.

We will present some of those setups here briefly.

The whole discussion can be read in our original German book or can be requested from the authors.

9.1 Measurement of angular momentum directly on an actively circularly emitting antenna

Our first experimental setup was composed of an $X - Quad$ suspended by a thin thread which was fed through very thin coaxial cables. Unfortunately the warming of the cables by electric current caused a random, incalculable disturbing torque on the antenna.

Thus we decided to mount a high capacity battery directly at the axis of the antenna. But the relation of transmitting power to the moment of inertia of the whole system combined with the instable thread suspension proved too unresponsive.

These problems could possibly be alleviated by a specially designed and constructed battery-powered transmitting system.

9.2 Measurement of angular momentum on a radiation absorbing disc

Next we tried to measure the angular momentum respectively torque on a radiation absorbing plate which was irradiated with a circular polarized radio wave.

The plate was made of absorption tiles Eccosorb of the firm Emerson und Cuming, USA and was suspended below the transmitting antenna.

The moment of inertia of the very heavy plate however proved to be too high for sensible experimental conditions.

This problem could possibly be alleviated by much higher transmitting powers.

9.3 Measurement of angular momentum on a thin metal disc by generation of circular polarized radiation by reflection

Under oblique incidence on a metal surface (see [1], [7] and [8]) a linear polarized wave with inclined polarization plane will be reflected partially circular polarized. A metal reflection disc thus should receive an angular momentum equal to that of the photons of the circular polarized reflected wave.

This offers the possibility to use a thin and lightweight metal disc instead of the heavy absorption tiles. In order to get approximately ideal reflection conditions the reflection plane must be greater than the wave length.

We therefore laid a large-area wire mesh on the ground and placed closely above that an aluminum disc suspended by a thread. Thus the metal disc and metal wires formed an almost homogenous plane without edge radiation respectively scattering by the metal disc.

The disc diameter was 60cm and the antenna we used was a linear polarized transmitting antenna with 6m wave length of the firm HyGain, USA, the huge dimensions however being a difficult experimental setup.

Unfortunately we had to realize that the accuracy of measurement was not satisfying.

However we could never find any evidence of an angular momentum transmitted to the disc.

9.4 Measurement of angular momentum on satellites by circular polarized emitting satellite antennas

As described in chapter 8, a measurement of the angular momentum of a specifically designed satellite with a high energy circular polarized transmitting antenna would be a very effective experiment. Apparently this would be very expensive, too.

10 Abstract

1. Our intention was to measure the spin of very low energy photons.

Therefore we had to use the photons of radio waves and to rely on macroscopic measurements of the spin. This means the transfer of the photon spin of a beam of polarized photons to a macroscopic object.

Our experiment concentrated on low energy photons of radio waves with $2.0m$ and $0.7m$ wave lengths. The transference of the angular momentum of the photons onto a small thin metal disc was accomplished by scattering of radio waves incident on the disc.

The radio waves were circular polarized corresponding to polarized photons in the photon conception.

Result:

On low energy photons in the range of radio waves there is no photon spin of magnitude $h/2\pi$ detectable.

Especially the experiments with the $2m$ -wave indicate that the photon spin at these wave lengths (if existent) is far below the value of $h/2\pi$.

2. The radiation of the transmitting antennas of satellites radiating circular polarized waves and their influence on the attitude dynamics has been analyzed.

If the spin of the radiated photons is frequency independent, perturbing torques on the satellites should have been detected.

Result:

No perturbing torques of this origin have been found even though these should be well accessible to common satellite measurement techniques.

This fact is a further indication for the assumption of a frequency dependent photon spin.

11 Addendum 1: Test records

All data refer to the deviation of the laser beam in meters standardized to $1m$ radius. (This corresponds at the same time to the double angle of rotation of the aluminum disc in radian measure.) In addition the corresponding standard deviation σ is indicated.

- Measurement at $2m$ wave length with an antenna height of $3m$:

0,0050	0
0,0043	0,0029
-0,0070	0
0	0,0045
0,0050	0,0050
-0,0040	-0,0150
-0,0120	0
-0,0067	0
-0,0070	0,0100
-0,002	-0,0110
-0,0130	0,0150
0,0090	0,0010
0,0040	

⇒ arithmetic mean: $0,0005 \pm 0,0074$

- Measurement at $2m$ wave length with an antenna height of $4.5m$:

-0,0008
0,0050
0,0025
-0,0100
-0,0010
0,0020

⇒ arithmetic mean: $0,0004 \pm 0,0048$

- Measurement at $70cm$ wave length with an antenna height of $5m$:

0
0,0050
-0,0083
0
0
0
0,0020

⇒ arithmetic mean: $0,0002 \pm 0,0037$

12 Addendum 2

12.1 Calculation of the angular momentum of the scattered radiation and the associated reactive opposed angular momentum respectively torsional moment of the scattering disc

To begin with, it should be stressed once more that our experiments and considerations deal with the real photons in the far field. The polarization degree of the dipole radiation depends on the angle of radiation. Correspondingly in the photon conception the spin of the scattered radiation varies with respect to the direction of radiation respectively the angle of radiation.

To sum up, in order to calculate the torsional moment onto the disc in the direction of the transmitting axis effected by the whole scattered radiation one has to determine the intensity of the scattered radiation depending on the angle of radiation, to weight this with its respective polarization degree, to project the resulting angular momentum of the individual rays on the transmitting axis and to integrate this angular momentum over the whole sphere.

The scattered radiation in projection on the plane of the metal disc is rotationally symmetric to the transmitting axis because the radiation can be represented by the superposition of two 90°-phase-delayed transmitting dipoles perpendicular to each other.

Now we apply the well known Poynting vector formalism $\vec{S} = \vec{E} \times \vec{H}$.

Let \vec{S} be the standard time dependent Poynting vector. We will use from now on a time-averaged Poynting vector $\vec{S} := \frac{1}{T} \int_0^T \vec{S} dt = \frac{1}{2} \cdot \vec{S}_0$. Hereby \vec{S}_0 is the peak value of \vec{S} .

As especially measurements of power and torsional moment respectively angular momentum refer to the time-averaged value in current practice we will further on use only this time-averaged value Poynting vector.

The calculation is carried through as usual for a sufficiently large radius R under far-field conditions, so that \vec{E} and \vec{H} are orthogonal to each other and \vec{S} is perpendicular to the surface of the sphere defined by R (see Fig. 12.1).

The absolute value of the Poynting vector of dipole I is maximal if orthogonal to the dipole, diminishes with smaller α and vanishes at last along the dipoles axis with $\alpha = 0$.

We name the maximal absolute value of the time-averaged Poynting vector \vec{S}_1 of the dipole antenna I (orthogonal to the dipole axis) $S_{max,1}$.

Then holds: $|\vec{S}_1| = S_{max,1} \cdot \sin^2 \alpha$

Since the field strength varies according to the well known formula for the radiation pattern of the dipole with $\sin \alpha$, the magnitude of the vector \vec{S} varies with $\sin^2 \alpha$, see [1], [8] or [9]).

By analogy we name the maximal absolute value of the time-averaged Poynting vector of the dipole antenna II (orthogonal to the dipole axis) $S_{max,2}$.

In our case of two orthogonally crossed dipole antennas we consider at first as a special case those two Poynting vectors of dipoles I and II which are at right angles to the plane defined by the two dipoles and overlap with the transmitting axis.

Here the magnitudes of those Poynting vectors add directly leading to the twofold radiation power density compared to the solitary dipole antennas.

We now have to determine the time-averaged Poynting vector $|\vec{S}_{ges}|$ of both antennas respectively the radiation power density of the dipole system for an arbitrary direction of radiation.

Let \vec{S}_{ges} be the total averaged radiation energy flux density respectively radiation power density in the direction of \vec{S} .

We consider at first only the coloured plane in 12.1 orthogonal to dipole II along dipole I.

Here the magnitude of the total time-averaged Poynting vector is composed of the magnitudes of the time-averaged Poynting vectors of both antennas in the following manner:

$$|\vec{S}_{ges}| = S_{max,1} \sin^2 \alpha + S_{max,2}$$

This consideration holds true for the coloured plane but beyond that due to the rotational radiation symmetry of the dipole system with regard to the transmitting axis and due to $S_{max,1} = S_{max,2} := S^*$ for all other directions likewise:

$$|\vec{S}_{ges}| = S^* \sin^2 \alpha + S^* \quad (12.1)$$

As one can immediately see this formula yields the right results for the special cases $\alpha = 0^\circ$ and $\alpha = 90^\circ$.

In order to determine the total radiated power W of the dipole system over the whole sphere one has to integrate the radiation energy flux density \vec{S} over the whole sphere with radius R :

$$\begin{aligned} W &= \oint_K (S^* \sin^2 \alpha + S^*) dA = S^* \int_{\alpha=-\frac{\pi}{2}}^{\frac{\pi}{2}} \int_{\phi=0}^{2\pi} (\sin^2 \alpha + 1) \cos \alpha R^2 d\phi d\alpha \\ &= S^* \cdot 2\pi R^2 \int_{\alpha=-\frac{\pi}{2}}^{\frac{\pi}{2}} (\sin^2 \alpha + 1) \cos \alpha d\alpha \\ &= 2\pi R^2 S^* \left[\sin \alpha + \frac{1}{3} \sin^3 \alpha \right]_{\alpha=-\frac{\pi}{2}}^{\frac{\pi}{2}} \\ &= 2\pi R^2 S^* \left(1 + \frac{1}{3} - (-1 - \frac{1}{3}) \right) = 2\pi R^2 S^* \left(2 + \frac{2}{3} \right) = \frac{16\pi R^2}{3} S^* \end{aligned} \quad (12.2)$$

On the other hand in the photon conception the photon flux density \vec{P}_S into the direction \vec{S} is proportional to the energy flux density $|\vec{S}|$, thus it holds $\vec{P}_S = konst. \cdot \vec{S}$.

Because of $konst. = \frac{1}{h\nu}$ (see chapter 2, $p = L/h\nu$) it holds

$$\vec{P}_S = \frac{1}{h\nu} \cdot \vec{S}.$$

Finally we have to calculate the circular polarized portion of the radiation.

Here one has to regard that the radiation which is radiated orthogonal to both dipoles is totally circular polarized (polarization degree 1) and that the radiation delivered in the plane defined by both dipoles has no circular polarized part (polarization degree 0). With growing angle α the degree of polarization increases.

We inspect once more exemplarily the coloured plane of Fig. 12.1.

In order to derive the flux density of the angular momentum created by the photons from the photon flux density $|\vec{P}_S|$ one has to adjust $|\vec{P}_S|$ by the factor $\sin^2 \alpha$, since dipole I is only circular polarizing by that factor (see fig. 12.1).

On the whole the minor contribution of the power density $S^* \sin^2 \alpha$ of the dipole I determines half of the angular momentum active photon flux density. The other half is contributed by part of the dipole II radiation.

The residual radiation of the dipole II into the considered direction remains as linear polarized radiation without any contribution to the angular momentum.

Thus it holds

$$|\vec{p}_S| = \frac{1}{h\nu} \cdot 2S^* \sin^2 \alpha$$

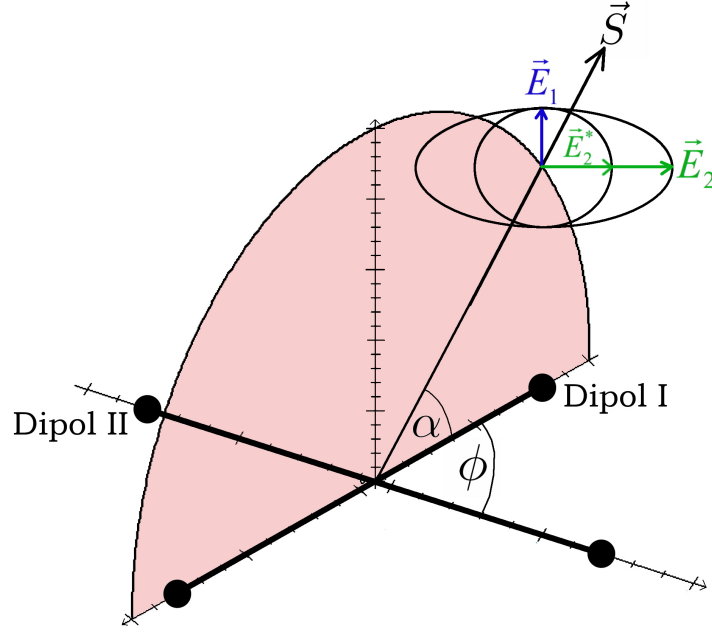


Figure 12.1: Construction of the polarization ellipse from field strength \vec{E}_1 of dipole I and field strength \vec{E}_2 of dipole II. \vec{E}_1 and \vec{E}_2 are 90° phase-delayed. The inscribed polarization circle, which determines the circular polarization of \vec{S} stems from \vec{E}_1 and $\vec{E}_2^* = \vec{E}_2 \cdot |\vec{E}_1|/|\vec{E}_2|$, which are accordingly 90° phase-delayed. The vector \vec{E}_2^* is part of \vec{E}_2 , leaving the rest of \vec{E}_2 for the linear polarized part of the radiation of \vec{S} .

with $\vec{p}_S :=$ angular momentum active photon flux density into direction \vec{S} .

Finally one has to take into account that only the component of the angular momentum along the transmitting axis contributes to the resultant total angular momentum of the disc. Those components orthogonal to the transmitting axis extinguish mutually because of the radiation symmetry.

Let \vec{j}_S be the angular momentum flux density into the direction \vec{S} . Then it holds: $\vec{j}_S = \frac{h}{2\pi} \vec{p}_S$ (see chapter 2).

Hence:

$$|\vec{j}_S| = \frac{h}{2\pi} \cdot \frac{1}{h\nu} \cdot 2S^* \sin^2 \alpha = \frac{1}{2\pi\nu} \cdot 2S^* \sin^2 \alpha$$

As mentioned above due to the rotation symmetry only the component into the direction of the transmitting axis remains affective.

In order to determine this component there is to calculate the projection $\vec{j}_{S,A}$ of \vec{j}_S onto the transmitting axis \vec{A} .

It holds:

$$|\vec{j}_{S,A}| = |\vec{j}_S| \cdot |\sin \alpha|$$

Hence:

$$|\vec{j}_{S,A}| = \frac{1}{2\pi\nu} \cdot 2S^* |\sin \alpha|^3$$

The total delivered angular momentum flux J_{ges} to the disc into the direction of the transmitting axis is therefore the following integral over the surface K of the sphere with radius R . (To notice is hereby that the projections of the spin contributions onto the transmitting axis having the same direction on both sides of the disc.) Therefore we integrate only over one half sphere and then double the value.

$$\begin{aligned}
J_{ges} &= 2 \cdot \oint_{K/2} \frac{1}{2\pi\nu} \cdot 2S^* \sin^3 \alpha \, dA \\
&= \frac{2S^*}{\pi\nu} \int_{\alpha=0}^{\frac{\pi}{2}} \int_{\phi=0}^{2\pi} \sin^3 \alpha \cos \alpha R^2 \, d\phi \, d\alpha \\
&= \frac{4S^*}{\nu} R^2 \int_{\alpha=0}^{\frac{\pi}{2}} \sin^3 \alpha \cos \alpha \, d\alpha \\
&= \frac{4S^*}{\nu} R^2 \left[\frac{1}{4} \sin^4 \alpha \right]_{\alpha=0}^{\frac{\pi}{2}} \\
&= \frac{S^* R^2}{\nu} \cdot 1 = \frac{S^* R^2}{\nu}
\end{aligned}$$

Since the total angular momentum flux J_{ges} of the scattered photons is equivalent to the angular momentum flux respectively torsional moment D_2 radiated from the disc, it holds:

$$D_2 = \frac{S^*}{\nu} R^2 \quad (12.3)$$

12.2 Resulting torsional moment on the disc

All in all there acts on the disc the torsional moment D_1 caused by the photons irradiated from the antenna less the torsional moment D_2 caused by the scattered photons.

Hence the resulting torsional moment on the disc is:

$$D = D_1 - D_2 = \frac{LA}{2\pi\nu} - \frac{S^*}{\nu} R^2$$

Furthermore one has to keep in mind that the total power scattered from the disc equals the irradiated radiation on the disc coming from the antenna (at least if one disregards the neglectible losses discribed in chapter 4.2.3).

Therefore according to formula 12.2 one can express S^* with the aid of L , for the total scattered power $W = \frac{16\pi}{3} S^* R^2$ equals the power LA incident from the antenna on the disc:

$$\frac{16\pi}{3} R^2 S^* = LA \quad \Rightarrow \quad S^* = \frac{3LA}{16\pi} \frac{1}{R^2}$$

Hence:

$$D = \frac{LA}{2\pi\nu} - \frac{3LA}{16\pi\nu} = \frac{LA}{2\pi\nu} \left(1 - \frac{3}{8}\right)$$

Consequently it holds:

$$\boxed{\text{resulting torsional moment } D = \frac{5}{8} \cdot \frac{LA}{2\pi\nu}} \quad (12.4)$$

13 Addendum 3

13.1 Proof of the equality of the geometrical area of the scattering disc in the photon conception and the effective area of the scattering disc in the electromagnetic wave conception

In the photon conception the photon stream and consequently the photon power incident on the disc is simply determined by the geometrical area of the disc. On the other hand there is the so called effective area used in the electromagnetic wave conception of antenna theory.

The effective area is the virtual area of which the antenna takes out the power of the electromagnetic wave.

In order to present an equivalent formulation of the scattering mechanism of both the photon and the electromagnetic conception we therefore have to prove that the geometrical area and the effective area of the disc are equal under the conditions of our experiment.

In the following we will derive the effective area of our disc by using solely the electromagnetic wave theory.

Therefore we have to examine the conditions, under which the incident electromagnetic wave interacts with the scattering metallic disc. To this end we calculate the resonant angular frequency ω_R of the disc by means of Thomson's resonant-oscillation-formula:

$$\omega_R = \frac{1}{\sqrt{L \cdot C}}$$

with L = inductance

C = capacitance

ω_R = resonant angular frequency $2\pi\nu$.

This angular resonant frequency of our disc compared with the frequency of the incident radiation of our transmitting antenna enables us to determine, which kind of scattering (Thomson- or resonance- or Rayleigh-scattering) takes place with the oscillating conduction electrons of our metal disc.

From this we can derive the effective cross section of the individual oscillating electrons and by summing them up we can determine the effective area of our disc.

Preliminary remarks on the determination of the inductance and capacity of the aluminum disc

In the following we use for our calculations a square of aluminum foil with side lengths 8cm instead of our round disc with diameter 9cm for simplification without loss of generality, thus the square and the disc offer the same area to the incoming radiation.

Thus we regard the square as a very flat short metal strap having an alternating voltage U_{AC} between its end faces with angular frequency ω_A (see fig. 4.3 and fig. 13.1).

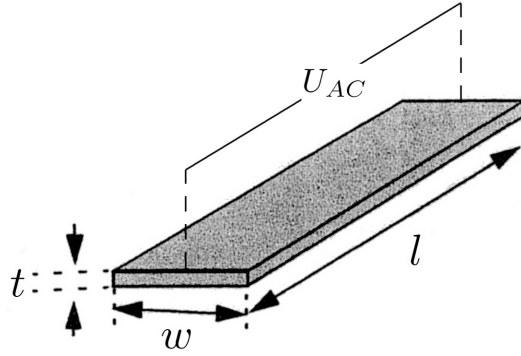


Figure 13.1: small metall strap

Hereby ω_A is the angular frequency of the electromagnetic wave of our transmitting antenna. The above mentioned voltage is caused by the electric field strength E_{AC} which in its return is produced by the incident wave coming from the antenna. Hence $U_{AC} = E_{AC} \cdot l$ with $l =$ length of the square.

Determination of the inductance L of the square

Treatises respectively textbooks on theoretical electromagnetism without reference to industrial development and practice do not supply sufficient information on the inductance of a straight metal strap as used in our experiment. So we had to refer to industrial technical knowledge. We use a formula used in many technical applications given by Microchip Incorporated Technology 2003:

$$L = 0,002l \cdot \left[\ln\left(\frac{2l}{w+t}\right) + 0,50049 + \frac{w+t}{3l} \right] \quad [\mu H]$$

with $w =$ width in cm
 $t =$ thickness in cm
 $l =$ length in cm .

Especially for our problem of the square it holds:

$w = 8cm$, $t = 0,0016cm$ and $l = 8cm$.

Therefrom it follows: $L = 25nH$

Another formula given by Mantaro Product Development Services, USA 2013, yields a very similar result.

Determination of the capacitance C of the square

As mentioned above the incident electromagnetic wave from the transmitting antenna induces an alternating current in the square which is defined by the inductance and the capacitance of the square. On the whole the square reacts in the manner of an oscillating antenna in the oscillating field of the incoming wave.

In order to calculate the capacitance C of the square we begin with the calculation of the capacitance of a straight wire with diameter and length equal to the thickness and length of the square, resembling a center-fed linear dipole antenna. The capacitance C (in free space) of our wire is

$$C = \frac{\pi\epsilon_0 h}{\ln(h/r)\sqrt{1/3}}$$

Hence $C = 0.22 \cdot 10^{-12}F$ with

$h =$ half length of the square respectively half length of the wire $= 0.04m$

$r =$ half thickness of the square respectively half diameter of the wire $= 0.008 \cdot 10^{-3}m$ (see [21]).

Herby we use

$$C = \frac{\pi\epsilon_0 h}{\ln(h/r)\sqrt{\frac{2d+l}{2d+3l}}}$$

with $d =$ gap between the inner terminals of the arms of the antenna and take the limit $d \rightarrow 0$ for the calculation of C .

We refer also to a corresponding approximation formula

$$C = \frac{\pi \epsilon_0 h}{\ln(h/r)}$$

given by [22].

The difference of his results to Gonschorek's in the context of our investigation is as we will explain below of negligible difference (factor 1.3), taking into account that the resonance angular frequency of our square is proportional to $1/\sqrt{C}$.

In the end our consideration on the capacitance of our square is governed simply by the question if the resonance frequency of the square lies in the range of the Thomson scattering range. Both formulas yield results clearly satisfying this condition.

Next we have to sum up such wires but with quadratic cross section side by side in order to get the configuration of a square. (The capacitance of such edged wires can be calculated to $C_q = 0.23 \cdot 10^{-12} F$ taking the capacitance of round wires with the same cross section.)

The necessary number of such wires is $s = l/d = 5 \cdot 10^3$.

Capacitances in parallel arrangement simply add up if the individual capacitances do not influence each other. In our special case the sum of capacitances of our parallel oriented wires adjacent to each other must be adjusted by the factor 1/2, because half of the lateral surfaces of the individual wires are neutralized mutually by direct metallic contact.

Thus it holds for the total capacity of the square:

$$C_T = s \cdot C_q \cdot 1/2 = 0.58 \cdot 10^{-12} F$$

with $C_q =$ capacity of an individual wire.

(The relative contribution of the narrow end faces of the square to its total capacitance can be neglected compared to its great total surface.)

Finally we have to take into consideration additional factors which influence the capacitance of our disc: First the capacitance produced by the edges of the disc and second the relative permittivity of the water film and the ceramic plate on which the disc is positioned.

The capacitance produced by the edges of the disc is some sort of capacitance „top loading” as it is called in antenna engineering.

The relative permittivity ϵ_r of water and ceramic plate on the bottom side of the disc certainly cause an important contribution to the capacitance of the disc.

All these contributions are characterized by the fact, that they increase additionally the whole capacitance of the disc. These factors are difficult to quantify, but it is not necessary to do this: Because above all every increase of the capacitance of the disc respectively our square will decrease the resonance frequency of the disc. In this way the resonance frequency will shift even more into the region of the Thomson scattering as will be shown later.

Thus these influences on the capacitance will but strengthen our argument of the equality of the effective and geometric area of the square which demands a resonance frequency in the Thomson scattering range. In the following we therefore can take the value of $C = 0.58 \cdot 10^{-12} F$ as a very reliable upper limit for our further calculations.

Determination of the upper limit ω_R of the angular resonance frequency of the square

According to Thomson's formula the angular resonance frequency $\omega_R = \frac{1}{\sqrt{LC}}$ ($L = 25 \cdot 10^{-9} H$ and $C = 0.58 \cdot 10^{-12} F$) of our square is $\omega_R = 263 \cdot 10^6 \text{ 1/sec}$.

In order to apply this result for the determination of the effective area F_{eff} of our square we have to compare the angular frequency ω_A of the incident wave coming from the antenna with the resonance frequency ω_R of the square.

From the scattering cross section to the the effective area of the square and our aluminum disc

Let us inspect the conditions of scattering and the scattering cross section of the conduction electrons of the metallic square. We refer to [12].

The scattering of the incident wave from our transmitting antenna by the conduction electrons of our aluminum disc is governed by the Thomson scattering principle. In this case the frequency of the incoming wave is much greater than the resonance frequency ω_R of the square respectively the associated equal frequency of the conduction electrons in the metal under condition of resonance.

In Thomson scattering the scattering cross sections σ_E of the individual conduction electrons oscillating synchronously under the influence of the incoming wave with ω_A are constant with respect to ω_A and ω_R : $\sigma_E = \text{const}_E$.

(In the ideal case for $\omega_A \gg \omega_R$ respectively for total free electrons without any restoring force there holds the classical Thomson scattering cross section $\sigma = \frac{8\pi}{3}R^2$ with $R =$ classical electron radius.

In our case the restoring force for the conduction electrons in the resonating square is negligible in consideration of the very low resonance frequency ω_R with $\omega_R < \omega_A$.

So we regard the conduction electrons of our square approximately as free in the context of our experiment.)

It should be stressed that Thomson scattering does not depend on the dimension of our metal square but only on its resonance frequency respectively its corresponding wave length, which can exceed many times the dimension of the plate. This wave length has to be compared with the length of the incoming wave to see if the Thomson scattering applies.

Now the total scattering cross section σ_T of a metal plate consists of the sum of the individual cross sections σ_E of the oscillating conduction electrons of the plate.

So using the Thomson scattering we can represent the total scattering cross section σ_T of a scattering metallic area by the formula $\sigma_T = \text{const}_T \cdot \text{geometrical area of the scattering disc } F_{\text{geometric}}$.

Since σ_T in terms of electromagnetic antenna theory is the effective area F_{eff} , we can write: $F_{\text{eff}} = \text{const}_T \cdot F_{\text{geometric}}$.

This formula holds for all pairs of F_{eff} and $F_{\text{geometric}}$ that obey the Thomson scattering condition.

We now have to determine the value of this constant.

If we know its value for some known geometric area $F_{\text{geometric}}^*$ we have as well the value for every other $F_{\text{geometric}}$, for the constant is the same for all pairs of F_{eff} and $F_{\text{geometric}}$.

In order to obtain the value of this constant we hence refer to practical knowledge of antenna engineering that holds for all well conducting metals.

We know by experience that with plane aerials (also known as flat top antennas) of dimensions much greater than the wave length of the incoming wave our constant equals 1, for in this case the relation $F_{\text{eff}} = F_{\text{geometric}}$ is valid (see [3].)

Therefore $F_{\text{eff}} = F_{\text{geometric}}$ is true for all metallic scattering plane areas that obey the Thomson condition.

Now let us return to our special problem, namely the scattering of the electromagnetic wave of our antenna by our aluminum disc.

Here the angular frequency ω_A of the incident wave is much greater than the resonance frequency ω_R of the square. In our case:

For the 2.1m-Antenna: $\omega_A = 905 \cdot 10^6 \text{ 1/sec}$

For the 0.68m-Antenna: $\omega_A = 2770 \cdot 10^6 \text{ 1/sec}$

For comparison: $\omega_R \leq 260 \cdot 10^6 \text{ 1/sec}$.

Therefore $F_{\text{eff}} = F_{\text{geometric}}$ for our scattering square under the conditions of our experiment.

Now on grounds of above considerations we also see that in terms of Thomson scattering the smallest dimension of the scattering metal plate is essential, not its shape.

So for our circular aluminum disc there holds the same condition: $F_{\text{eff}} = F_{\text{geometric}}$

References

- [1] Pohl, R.W.: *Optik und Atomphysik*, Springer, Berlin 1958
- [2] Demtröder, W.: *Experimentalphysik - Elektrizität und Optik*, Springer, Berlin 2004
- [3] Meinke, Gundlach: *Taschenbuch der Hochfrequenztechnik Band 2*, Springer, Berlin 1992
- [4] Straw R.D. : *The ARRL Antenna Book*, ARRL, Newington 2005
- [5] Bergmann, L., Schäfer, Cl.: *Lehrbuch der Experimentalphysik Band 2 - Elektromagnetismus*, deGruyter, Berlin 1999
- [6] Bergmann, L., Schäfer, Cl.: *Lehrbuch der Experimentalphysik Band 3 - Optik, Wellen- und Teilchenoptik*, Springer, Berlin 2004
- [7] Born, M.: *Optik*, Springer, Berlin 1985
- [8] Schäfer, Cl.: *Einführung in die theoretische Physik Band 3 - Elektromagnetismus und Optik*, deGruyter, Berlin 1961
- [9] Bergmann, L., Schäfer, Cl.: *Lehrbuch der Experimentalphysik Band 2 - Elektrizitätslehre*, Springer, Berlin 1961
- [10] Dasgupta, R., Gupta, P.K.: *Rotation of transparent, non-birefringent objects by transfer of optical spin angular momentum*, CAT Newsletter Vol.18, Indore 2005
- [11] Courant, R.: *Vorlesungen über Differential- und Integralrechnung Band 2*, Springer, Berlin 1958
- [12] Slater, J.S., Frank, N.H.: : *Electromagnetism*, Dover, New York 1969
- [13] Rothammel, K.: *Antennenbuch*, Militärverlag der DDR, Berlin 1984
- [14] Johnson, R.C.: *Antenna Engineering Handbook*, McGraw-Hill, New York 1993
- [15] Kruesi, W.R., Howell, I.H: *IEEE Standard Test Procedures For Antennas*, Wiley, 1979
- [16] Capps, C.: *Near field or far field*, EDE Magazine (Electronics Design Engineers), 2001
- [17] Hughes, P.C.: *Spacecraft Attitude Dynamics*, Dover, New York 2001
- [18] Ley, W., Hallmann, W. (Hrsg): *Handbuch der Raumfahrttechnik*, Hanser, Berlin 2004

- [19] Steiner, W., Schagerl, M.: *Raumflugmechanik*, Springer, Berlin 2004
- [20] Pattan, B.: *Satellite Systems, Principles and Technologies*, Hall, New York 1993
- [21] V.H.Gonschorek: *EMV für Geräteentwickler und Systemintegratoren*, Springer, Berlin - New York 2005
- [22] K.T. McDonald, Joseph Henry Laboratories, Princeton University, USA 2012